Eur. Phys. J. D **13**, 33–41 (2001)

**THE EUROPEAN PHYSICAL JOURNAL D**

EDP Sciences


# Binding energies and scattering observables in the $^4He_3$ atomic system

A.K. Motovilov[1,a], W. Sandhas[1], S.A. Sofianos[2], and E.A. Kolganova[3]

[1] Physikalisches Institut der Universität Bonn, Endenicher Allee 11-13, 53115 Bonn, Germany
[2] Physics Department, University of South Africa, P.O. Box 392, Pretoria 0003, South Africa
[3] Joint Institute for Nuclear Research, Dubna 141980, Russia

Received 19 June 2000

**Abstract.** The $^4He_3$ system is investigated using a hard-core version of the Faddeev differential equations. Realistic $^4$He–$^4$He interactions are employed, among them the LM2M2 potential by Aziz and Slaman and the recent TTY potential by Tang, Toennies and Yiu. We calculate the binding energies of the $^4$He trimer, but concentrate in particular on scattering observables. The scattering lengths and the atom-diatom phase shifts are calculated for center of mass energies up to 2.45 mK. It is found that the LM2M2 and TTY potentials, although of quite different structure, give practically the same bound-state and scattering results.

**PACS.** 02.60.Nm Integral and integrodifferential equations – 21.45.+v Few-body systems

## 1 Introduction

Studies of small $^4$He clusters (in particular dimers and trimers) represent an important step towards understanding the properties of helium liquid drops, super-fluidity in $^4$He films, the Bose-Einstein condensation etc. (see, for instance, Refs. [1–4]). Besides, the helium trimer is probably a first specific molecular system where a direct manifestation of the Efimov effect [5] can be observed, for the binding energy $\epsilon_d$ of the $^4$He dimer is extremely small (about 1 mK) on the molecular scale.

There is a great number of experimental and theoretical investigations of $^4$He clusters. Out of the experimental works we mention references [6–11] where molecular clusters of helium and other noble gas atoms were considered. Most of the theoretical investigations consist in computing the ground-state energy and are based on variational methods [12–17], on hyperspherical harmonics expansions in configuration space [18,19], and on integral equations in momentum space [20,21]. We further note that the results of reference [22] were based on a direct solution of the two-dimensional Faddeev differential equations in configuration space, while recently binding-energy results were obtained by using the three-dimensional Faddeev differential equations in the total-angular-momentum representation [23]. A qualitative treatment of the $^4He_3$ system in an effective field theory is presented in reference [24]. In references [17,18,21,25] it was shown that the excited state of the $^4$He trimer is indeed an Efimov state [5]. Another proof of the Efimov nature of the excited state of the trimer, based on a scaling consideration, is discussed in [26]. The resonance mechanism of formation and disappearance of the Efimov levels in the $^4He_3$ system has been studied in references [27,28]. A very promising experimental method for determining the excited state of the $^4$He trimer is suggested in a recent paper [29].

In contrast to the bulk of theoretical investigations devoted to the binding energies of the $^4$He trimer, scattering processes found comparatively little attention. In reference [20] the characteristics of the He–$He_2$ scattering at zero energy were studied, while the recombination rate of the reaction $(1+1+1 \to 2+1)$ was estimated in [30]. The phase shifts of the He–$He_2$ elastic scattering and breakup amplitudes at ultra-low energies have been calculated for the first time just recently in [25] (see also [31,32]) and this was only done for the comparatively old HFD-B potential by Aziz *et al.* [33].

In principle, the problem of three helium atoms can be considered as an example of an ideal three-body quantum problem, since $^4$He atoms are identical neutral bosons and, thus, their handling is not complicated by spin, isospin, or Coulomb considerations. But, in fact, the $^4$He triatomic system belongs to the three-body systems whose theoretical treatment, regarding the excited states and scattering processes, is quite difficult. The difficulty is mainly due to two reasons. First, the low energy $\epsilon_d$ of the dimer makes

[a] On leave of absence from the Joint Institute for Nuclear Research, Dubna 141980, Russia.
e-mail: motovilv@thsun1.jinr.ru

it necessary to consider very large domains in configuration space with a characteristic size of hundreds of Ångstroems. Second, the strong repulsion of the He–He interaction at short distances produces large numerical errors.

In the present paper, which is an extension of the considerations of [25], we employ the mathematically rigorous hard-core version of the Faddeev differential equations of references [34,35]. This method overcomes the strong-repulsion problem just mentioned. As compared to [25] we use in the present work the refined He–He interatomic potentials LM2M2 by Aziz and Slaman [36], and TTY by Tang, Toennies, and Yiu [37]. Our numerical methods have also been substantially improved which allowed us to deal with considerably larger grids achieving, thus, a better accuracy. Furthermore, due to better computing facilities more partial waves were taken into account.

The paper is organized as follows. In Section 2 we shortly review the three-body bound and scattering state formalism for hard-core interactions. In Section 3 we describe numerical details of its application to the system of three $^4$He atoms. Our numerical results are presented in Section 4. Finally, in the Appendix we give details of the potentials used.

## 2 Formalism

In this work we employ a hard-core version of the Faddeev differential equation developed in [34,38]. It has also been described in detail in reference [25]. Therefore, in what follows we only outline the formalism and present its main characteristics needed for understanding our procedure.

In treating the three-body system we use the standard Jacobi coordinates $\mathbf{x}_\alpha, \mathbf{y}_\alpha$, $\alpha = 1,2,3$, expressed in terms of the position vectors of the particles $\mathbf{r}_i$ and their masses $\mathrm{m}_i$,

$$\mathbf{x}_\alpha = \left[\frac{2\mathrm{m}_\beta \mathrm{m}_\gamma}{\mathrm{m}_\beta + \mathrm{m}_\gamma}\right]^{1/2} (\mathbf{r}_\beta - \mathbf{r}_\gamma)$$

$$\mathbf{y}_\alpha = \left[\frac{2\mathrm{m}_\alpha(\mathrm{m}_\beta + \mathrm{m}_\gamma)}{\mathrm{m}_\alpha + \mathrm{m}_\beta + \mathrm{m}_\gamma}\right]^{1/2} \left(\mathbf{r}_\alpha - \frac{\mathrm{m}_\beta \mathbf{r}_\beta + \mathrm{m}_\gamma \mathbf{r}_\gamma}{\mathrm{m}_\beta + \mathrm{m}_\gamma}\right)$$

where $(\alpha, \beta, \gamma)$ stands for a cyclic permutation of the indices $(1,2,3)$. The coordinates $\mathbf{x}_\alpha, \mathbf{y}_\alpha$ fix the six-dimensional vector $X \equiv (\mathbf{x}_\alpha, \mathbf{y}_\alpha) \in \mathbb{R}^6$. By $\Delta_X$ we denote Laplacian in $X$.

In the hard-core potential model one requires the three-body wave function $\Psi(X)$ to vanish when two of the three particles, say $\beta$ and $\gamma$, approach each other at distances $|\mathbf{x}_\alpha| \le c_\alpha$ where $c_\alpha$ is the hard-core radius in the channel $\alpha$, *i.e.*,

$$\Psi(X)|_{|\mathbf{x}_\alpha| \le c_\alpha} = 0, \qquad \alpha = 1,2,3\,. \tag{1}$$

One can show [35,38] that in this model the Faddeev components $\Phi_\alpha(X)$, $\alpha = 1,2,3$, satisfy the following system of differential equations

$$\begin{cases} (-\Delta_X + V_\alpha - E)\Phi_\alpha(X) = -V_\alpha \sum\limits_{\beta \ne \alpha} \Phi_\beta(X), & |\mathbf{x}_\alpha| > c_\alpha \\ (-\Delta_X - E)\Phi_\alpha(X) = 0, & |\mathbf{x}_\alpha| < c_\alpha \end{cases} \tag{2}$$

where $V_\alpha$ stands for the potential acting between particles $\beta$ and $\gamma$ outside the core domain, *i.e.*, at $|\mathbf{x}_\alpha| > c_\alpha$. Outside all the core domains the components $\Phi_\alpha$ provide the total wave function $\Psi$,

$$\sum_{\beta=1}^{3} \Phi_\beta(X)\Big|_{|\mathbf{x}_\alpha| > c_\alpha,\, \alpha=1,2,3} = \Psi(X)$$

while in the interior region we have, in accordance with (1),

$$\sum_{\beta=1}^{3} \Phi_\beta(X) \equiv 0, \qquad \alpha = 1,2,3.$$

In practice, one can replace the latter strong condition by a weaker one [34,38],

$$\sum_{\beta=1}^{3} \Phi_\beta(X)\Big|_{|\mathbf{x}_\alpha| = c_\alpha} = 0, \qquad \alpha = 1,2,3\,, \tag{3}$$

which requires the sum of $\Phi_\beta(X)$ to be zero only at the boundaries of the core domains.

The numerical advantage of our approach is already obvious from the structure of equations (2). When a potential with a strong repulsive core is replaced by the hard-core model, one approximates inside the core domains only the Laplacian $\Delta_X$ instead of the sum of the Laplacian and the huge repulsive term. In this way a much better numerical approximation is achieved.

In the present investigation we apply this formalism to the $^4$He three-atomic system with total angular momentum $L = 0$. The partial-wave version of equations (2) for a system of three identical bosons with $L = 0$ reads [39,40]

$$\left[-\frac{\partial^2}{\partial x^2} - \frac{\partial^2}{\partial y^2} + l(l+1)\left(\frac{1}{x^2} + \frac{1}{y^2}\right) - E\right]\Phi_l(x,y) = \begin{cases} -V(x)\Psi_l(x,y), & x > c \\ 0, & x < c\,. \end{cases} \tag{4}$$

Here, $x, y$ are the absolute values of the Jacobi variables and $c$ is the core size, which is the same for all three two-body subsystems. The angular momentum $l$ corresponds to a dimer subsystem and a complementary atom. For a three-boson system in an $S$-state, $l$ can only be even, $l = 0,2,4,...$ The potential $V(x)$ is assumed to be central and the same for all partial waves $l$. The function $\Psi_l(x,y)$ is related to the partial-wave Faddeev components $\Phi_l(x,y)$ by

$$\Psi_l(x,y) = \Phi_l(x,y) + \sum_{l'} \int_{-1}^{+1} \mathrm{d}\eta\, h_{ll'}(x,y,\eta)\, \Phi_{l'}(x',y') \tag{5}$$

where

$$x' = \sqrt{\frac{1}{4}\,x^2 + \frac{3}{4}\,y^2 - \frac{\sqrt{3}}{2}\,xy\eta}\,,$$
$$y' = \sqrt{\frac{3}{4}\,x^2 + \frac{1}{4}\,y^2 + \frac{\sqrt{3}}{2}\,xy\eta}\,,$$

with $\eta = \hat{\mathbf{x}}\cdot\hat{\mathbf{y}}$. Analytic expressions for the kernels $h_{ll'}$ are found in [25,39,40]. It should be noted that these kernels depend only on the hyperangles

$$\theta = \arctan\frac{y}{x} \quad \text{and} \quad \theta' = \arctan\frac{y'}{x'}$$

but not on the hyperradius

$$\rho = \sqrt{x^2+y^2} = \sqrt{x'^2+y'^2}\,.$$

The functions $\Phi_l(x,y)$ satisfy the boundary conditions

$$\Phi_l(x,y)|_{x=0} = \Phi_l(x,y)\,|_{y=0} = 0\,. \tag{6}$$

The partial-wave version of the hard-core boundary condition (3) reads

$$\Phi_l(c,y) + \sum_{l'}\int_{-1}^{+1} \mathrm{d}\eta\, h_{ll'}(c,y,\eta)\,\Phi_{l'}(x',y') = 0 \tag{7}$$

which requires the wave function $\Psi_l(x,y)$ to be zero at the core boundary $x = c$. Furthermore, one can show that, in general, condition (7) like condition (3) causes also the functions (5) to vanish inside the core domains.

The asymptotic condition for the helium trimer bound states reads [39]

$$\Phi_l(x,y) = \delta_{l0}\psi_{\mathrm{d}}(x)\exp(\mathrm{i}\sqrt{E_{\mathrm{t}}-\epsilon_{\mathrm{d}}}\,y)\left[a_0 + o\Big(y^{-1/2}\Big)\right] + \frac{\exp(\mathrm{i}\sqrt{E_{\mathrm{t}}}\rho)}{\sqrt{\rho}}\left[A_l(\theta) + o\Big(\rho^{-1/2}\Big)\right] \tag{8}$$

as $\rho\to\infty$ and/or $y\to\infty$. Here we use the fact that the helium dimer bound state exists only for $l = 0$. $\epsilon_{\mathrm{d}}$ stands for the dimer energy while $\psi_{\mathrm{d}}(x)$ denotes the dimer wave function which is assumed to be zero within the core, *i.e.*, $\psi_{\mathrm{d}}(x)\equiv 0$ for $x\le c$.

The coefficients $a_0$ and $A_l(\theta)$ describe the contributions of the $(2+1)$ and $(1+1+1)$ channels to $\Phi_l$, respectively. Both the trimer binding energy $E_{\mathrm{t}}$ and the difference $E_{\mathrm{t}}-\epsilon_{\mathrm{d}}$ in (8) are negative which means that for any $\theta$ the function $\Phi_l(x,y)$ decreases exponentially as $\rho\to\infty$.

The asymptotic boundary condition for the partial-wave Faddeev components of the $(2+1\to 2+1;\,1+1+1)$ scattering wave function reads for $\rho\to\infty$ and/or $y\to\infty$

$$\Phi_l(x,y;p) = \delta_{l0}\psi_{\mathrm{d}}(x)\left\{\sin(py) + \exp(\mathrm{i}py)\left[a_0(p) + o\Big(y^{-1/2}\Big)\right]\right\} + \frac{\exp(\mathrm{i}\sqrt{E}\rho)}{\sqrt{\rho}}\left[A_l(E,\theta) + o\Big(\rho^{-1/2}\Big)\right] \tag{9}$$

**Table 1.** Dimer energies $\epsilon_{\mathrm{d}}$, inverse wave lengths $1/\varkappa^{(2)}$, and $^4$He–$^4$He scattering lengths $\ell_{\mathrm{sc}}^{(2)}$ for the potentials used.

| Potential | $\epsilon_{\mathrm{d}}$ (mK) | $1/\varkappa^{(2)}$ (Å) | $\ell_{\mathrm{sc}}^{(2)}$ (Å) |
|---|---|---|---|
| HFDHE2 | −0.83012 | 120.83 | 124.65 |
| HFD-B | −1.68541 | 84.80 | 88.50 |
| LM2M2 | −1.30348 | 96.43 | 100.23 |
| TTY | −1.30962 | 96.20 | 100.01 |

where $p$ is the momentum corresponding to the variable $y$, $E$ is the scattering energy given by $E = \epsilon_{\mathrm{d}} + p^2$, and $a_0(p)$ is the elastic scattering amplitude. The functions $A_l(E,\theta)$ provide us for $E>0$ with the corresponding partial-wave breakup amplitudes.

The helium-atom helium-dimer scattering length $\ell_{\mathrm{sc}}$ is given by

$$\ell_{\mathrm{sc}} = -\frac{\sqrt{3}}{2}\lim_{p\,\to\,0}\frac{a_0(p)}{p}$$

while the $S$-state elastic scattering phase shifts $\delta_0(p)$ are given by

$$\delta_0(p) = \frac{1}{2}\,\mathrm{Im}\,\ln S_0(p). \tag{10}$$

Here $S_0(p) = 1+2\mathrm{i}\,a_0(p)$ is the $(2+1\to 2+1)$ partial-wave component of the scattering matrix.

## 3 Numerical details

As mentioned in the Introduction, an essential part of our present approach consists in a substantial improvement of our methods. Let us, therefore, go into some technical details. We employed the Faddeev equations (4) and the hard-core boundary condition (7) to calculate the binding energies of the helium trimer and the ultra-low energy phase shifts of the helium atom scattered off the helium diatomic molecule. As He–He interaction we used three versions of the semi-empirical potentials of Aziz and collaborators, namely HFDHE2 [41], HFD-B [33], and the newer version LM2M2 [36]. Furthermore, we employed the latest theoretical He–He potential TTY of Tang *et al.* [37]. These potentials are given in the Appendix. In our calculations we used the value $\hbar^2/m = 12.12\ \mathrm{K\,Å^2}$. All the potentials considered produce a weakly bound dimer state. The energy $\epsilon_{\mathrm{d}}$ of this state together with the He–He atomic scattering length $\ell_{\mathrm{sc}}^{(2)}$ are given in Table 1. Notice that the latest potentials LM2M2 and TTY give practically the same scattering length $\ell_{\mathrm{sc}}$ and dimer energy $\epsilon_{\mathrm{d}}$.

A description of our numerical method has been given in reference [25]. Therefore, we outline here only the main steps of the computational scheme employed to solve the boundary-value problems (4, 6, 7) and (8) or (9). First, we note that the grid for the finite-difference approximation of the polar coordinates $\rho$ and $\theta$ is chosen such that the points of intersection of the arcs $\rho=\rho_i$, $i=1,2,...,N_\rho$ and

the rays $\theta = \theta_j$, $j = 1, 2, ..., N_\theta$ with the core boundary $x = c$ constitute the knots. We found that the values of the hard-core diameter $c$ of $^4$He atoms, taken within the interval 0.7–1.3 Å, provide a dimer bound-state energy $\epsilon_{\rm d}$ which is stable within six figures and a trimer ground-state energy $E_{\rm t}^{(0)}$ stable at least within three figures. The reason of such a stability is simple: even the radius 2 Å lies in the highly repulsive domain of the He–He potential. For example, the value of the LM2M2 potential for this radius is 538 K while for 1.5 Å it acquires the value of 5 590 K. Thus, in the present work we were allowed to fix the core diameter $c$ to be simply 1.0 Å. The $\rho_i$ are chosen according to

$$\rho_i = \frac{i}{N_c^{(\rho)} + 1}\, c, \qquad i = 1, 2, ..., N_c^{(\rho)},$$
$$\rho_{i+N_c^{(\rho)}} = \sqrt{c^2 + y_i^2}, \qquad i = 1, 2, ..., N_\rho - N_c^{(\rho)},$$

where $N_c^{(\rho)}$ stands for the number of arcs inside the domain $\rho < c$ and

$$y_i = f(\tau_i)\sqrt{\rho_{N_\rho}^2 - c^2}, \qquad \tau_i = \frac{i}{N_\rho - N_c^{(\rho)}}.$$

The nonlinear monotonously increasing function $f(\tau)$, $0 \leq \tau \leq 1$, satisfying the conditions $f(0) = 0$ and $f(1) = 1$, is chosen to be

$$f(\tau) = \begin{cases} \alpha_0 \tau & , \tau \in [0, \tau_0] \\ \alpha_1 \tau + \tau^\nu & , \tau \in (\tau_0, 1] \end{cases}.$$

The values of $\alpha_0$, $\alpha_0 \geq 0$, and $\alpha_1$, $\alpha_1 \geq 0$, are determined *via* $\tau_0$ and $\nu$ from the continuity condition for $f(\tau)$ and its derivative at the point $\tau_0$. In the present investigation we took values of $\tau_0$ within 0.15 and 0.2. The value of the power $\nu$ depends on the cutoff radius $\rho_{\max} = \rho_{N_\rho} = 200$–1 000 Å, its range being within 3.4 and 4 in the present calculations.

The knots $\theta_j$ at $j = 1, 2, ..., N_\rho - N_c^{(\rho)}$ are taken according to $\theta_j = \arctan(y_j/c)$ with the remaining knots $\theta_j$, $j = N_\rho - N_c^{(\rho)} + 1, ..., N_\theta$, being chosen equidistantly. Such a choice is required by the need of having a higher density of points in the domain where the functions $\Phi_l(x, y; z)$ change most rapidly, *i.e.*, for small values of $\rho$ and/or $x$. In this work, we used grids of the dimension $N_\theta = N_\rho = 500$–800 while the above number $N_c^{(\rho)}$ and the number $N_\theta - (N_\rho - N_c^{(\rho)})$ of knots in $\theta$ lying in the last arc inside the core domain was chosen equal to 2–5.

Since we consider identical bosons, only the components $\Phi_l$ corresponding to even $l$ differ from zero. Thus, the number of equations to be solved is $N_{\rm e} = l_{\max}/2 + 1$ where $l_{\max}$ is the maximal even partial wave. The finite-difference approximation of the $N_{\rm e}$ equations (4) reduces the problem to a system of $N_{\rm e} N_\theta N_\rho$ linear algebraic equations. The finite-difference equations corresponding to the arc $i = N_\rho$ include initially the values of the unknown functions $\Phi_l(x, y; z)$ from the arc $i = N_\rho + 1$. To eliminate them, we express these values through the values of $\Phi_l(x, y; z)$ on the arcs $i = N_\rho$ and $i = N_\rho - 1$ by using the asymptotic formulas (8) or (9) in the manner described in the final part of Appendix A of reference [25]. In [25], however, this approach was used for computing the binding energies only, while in the present work this method is extended also to the scattering problem. The matrix of the resulting system of equations has a block three-diagonal form. Every block has the dimension $N_{\rm e} N_\theta \times N_{\rm e} N_\theta$ and consists of the coefficients standing at unknown values of the Faddeev components in the grid knots belonging to a certain arc $\rho = \rho_i$. The main diagonal of the matrix consists of $N_\rho$ such blocks.

In this work we solve the block three-diagonal algebraic system on the basis of the matrix sweep method [42]. This method makes it possible to avoid using disk storage for the matrix during the computation. Besides, the matrix sweep method reduces the computer time required by almost one order of magnitude as compared to [25].

## 4 Results

Our results for the trimer ground-state energy $E_{\rm t}^{(0)}$, as well as the results obtained by other authors, are presented in Table 2. It should be noted that most of the contribution to the ground-state energy stems from the $l = 0$ and $l = 2$ partial-wave components, the latter being slightly more than 30%, and is approximately the same for all potentials used. The contribution from the $l = 4$ partial wave is of the order of 3–4% (*cf.* [22]). One can see that our results for $E_{\rm t}^{(0)}$ with $l_{\max} = 4$ are in perfect agreement with corresponding values obtained in the most advanced calculations [12–16,19,23]. Our ground-state energy $E_{\rm t}^{(0)}$ for LM2M2 disagrees, however, with the variational value $-0.15$ cm$^{-1}$ $= -0.216$ K for $E_{\rm t}^{(0)}$ obtained with the same potential in [17] (here, for converting the energy units we use the factor 1 cm$^{-1}$ $= 1.4387752$ K [43]).

The results obtained for the excited-state energy of the trimer $E_{\rm t}^{(1)}$, as well as the results found in the literature, are presented in Table 3. To illustrate the convergence of our results, we show in Table 4 the dependence of $E_{\rm t}^{(1)}$ on the grid parameters using the TTY potential. It is seen that the $l = 0$ partial-wave component contributes about 71% to the excited-state binding energy. The contribution to $E_{\rm t}^{(1)}$ from the $l = 2$ component is about 25–26% and from $l = 4$ within 3–4%. These values are similar to the ones for the ground state. Finally, we see that our results for $E_{\rm t}^{(1)}$ are in a quite good agreement with the best results for $E_{\rm t}^{(1)}$ found in the literature [19,23], while they deviate considerably from the result $E_{\rm t}^{(1)} = -1.24 \times 10^{-3}$ cm$^{-1}$ $=$ $-1.784$ mK of reference [17] obtained with LM2M2.

Although we have performed detailed calculations of the $^4$He$_3$ binding energies, the main goal of the present work was to perform calculations for the scattering of a helium atom off a helium dimer at ultra-low energies. Our results at $L = 0$ for the scattering length of the collision of the He atom on the He dimer, obtained for the HFD-B, LM2M2 and TTY potentials, are presented

**Table 2.** Ground state energies $E_t^{(0)}$ for the helium trimer obtained *via* different methods. The (absolute) values of $E_t^{(0)}$ are given in K. The grid parameters used were $N_\theta = N_\rho = 555$, $\tau_0 = 0.2$, $\nu = 3.6$, and $\rho_{\max} = 250$ Å.

| | | Faddeev equations | | | | | Variational methods | | | | | Adiabatic approaches | |
|---|---|---|---|---|---|---|---|---|---|---|---|---|---|
| Potential | $l_{\max}$ | this work | | [22] | [21] | [20] | [23] | [13] | [12] | [14] | [15] | [16] | [18] | [19] |
| HFDHE2 | 0 | $0.084^{(a)}$ | 0.0823 | | 0.082 | 0.092 | | | | | | | 0.098 | |
| | 2 | $0.114^{(a)}$ | 0.1124 | 0.107 | 0.11 | | | | | | | | | |
| | 4 | 0.1167 | | | | | 0.1171 | 0.1173 | | | | | | |
| HFD-B | 0 | $0.096^{(a)}$ | 0.0942 | 0.096 | | | | | | | | | | |
| | 2 | $0.131^{(a)}$ | 0.1277 | 0.130 | | | | | | | | | | |
| | 4 | 0.1325 | | | | | 0.1330 | | 0.1193 | 0.133 | 0.131 | 0.129 | | |
| LM2M2 | 0 | 0.0891 | | | | | | | | | | | 0.106 | |
| | 2 | 0.1213 | | | | | | | | | | | | |
| | 4 | 0.1259 | | | | | 0.1264 | | | | | | | 0.1252 |
| TTY | 0 | 0.0890 | | | | | | | | | | | | |
| | 2 | 0.1212 | | | | | | | | | | | | |
| | 4 | 0.1258 | | | | | 0.1264 | | | | 0.126 | | | |

$^{(a)}$Results from [25] for a grid with $N_\theta = N_\rho = 275$ and $\rho_{\max} = 60$ Å.

**Table 3.** Excited state energies $E_t^{(1)}$ for the helium trimer. The (absolute) values of $E_t^{(1)}$ are given in mK. The grid parameters used were $N_\theta = N_\rho = 805$, $\tau_0 = 0.2$, $\nu_0 = 3.6$, and $\rho_{\max} = 300$ Å.

| Potential | $l_{\max}$ | this work | | [21] | [20] | [23] | [18] | [19] |
|---|---|---|---|---|---|---|---|---|
| HFDHE2 | 0 | $1.5^{(a)}$ | 1.46 | 1.46 | 1.04 | | 1.517 | |
| | 2 | $1.7^{(a)}$ | 1.65 | 1.6 | | | | |
| | 4 | 1.67 | | | | 1.665 | | |
| HFD-B | 0 | $2.5^{(a)}$ | 2.45 | | | | | |
| | 2 | $2.8^{(a)}$ | 2.71 | | | | | |
| | 4 | 2.74 | | | | 2.734 | | |
| LM2M2 | 0 | 2.02 | | | | | 2.118 | |
| | 2 | 2.25 | | | | | | |
| | 4 | 2.28 | | | | 2.271 | | 2.269 |
| TTY | 0 | 2.02 | | | | | | |
| | 2 | 2.25 | | | | | | |
| | 4 | 2.28 | | | | 2.280 | | |

$^{(a)}$Results from [25] for a grid with $N_\theta = N_\rho = 252$ and $\rho_{\max} = 250$ Å.

**Table 4.** Trimer excited-state energy $E_t^{(1)}$ (mK) obtained with the TTY potential for various grids.

| | $N_\theta = N_\rho = 252$ | $N_\theta = N_\rho = 502$ | $N_\theta = N_\rho = 652$ |
|---|---|---|---|
| $l_{\max}$ | $\rho_{\max} = 250$ Å | $\rho_{\max} = 300$ Å | $\rho_{\max} = 300$ Å |
| 0 | −2.108 | −2.039 | −2.029 |
| 2 | −2.348 | −2.273 | −2.258 |
| | $N_\theta = N_\rho = 805$ | $N_\theta = N_\rho = 1005$ | |
| $l_{\max}$ | $\rho_{\max} = 300$ Å | $\rho_{\max} = 300$ Å | |
| 0 | −2.024 | −2.021 | |
| 2 | −2.253 | −2.248 | |

in Table 5. For the definition of the scattering length, in case of at least one of the two particles being composite, see, *e.g.*, Section II B in reference [20]. Our approach to calculation of the He–$He_2$ scattering length is described in [25]. As compared to [25] the present calculation is essentially improved (the result $\ell_{sc} = 145 \pm 5$ Å for HFD-B with $l_{\max} = 2$ was obtained in [25] with a much smaller grid). Notice that the exact value of this length is important for estimating the three-body recombination rate of Bose-condensed helium atoms (see [30,44]). Apart from our previous result [25], there exist, to our knowledge, only two further results for the He–$He_2$ scattering length. The one of reference [20] provides $\ell_{sc} = 195$ Å, obtained within a zero-energy scattering calculation based on a separable approximation for the oldest Aziz *et al.* He–He potential HFDHE2. A more recent one is obtained by Blume and Greene [45] *via* a Monte Carlo hyperspherical calculations with the LM2M2 potential. Their result of $\ell_{sc} = 126$ Å is in good agreement with our result of $131 \pm 5$ Å (see Tab. 5). Within the accuracy of our calculations, the scattering lengths provided by the LM2M2 and TTY potentials, like the energies of the excited state, are exactly the same. It should be mentioned that in this case also the two-body binding energies and scattering lengths are almost indentical.

The phase shifts obtained for the HFD-B, LM2M2 and TTY potentials are given in Tables 6–8. For the HFD-B and TTY potentials they are plotted in Figure 1. Note that for the phase shifts we use the normalization required by the Levinson theorem [46], $\delta_L(0) - \delta_L(\infty) = n\pi$, where $n$ is the number of trimer bound states. Incident energies below and above the breakup threshold, *i.e.* for the processes $(2+1 \longrightarrow 2+1)$ and $(2+1 \longrightarrow 1+1+1)$, were considered. It was found that after transformation to the laboratory system the phase shifts $\delta_0^{(l_{\max})}$ for the potentials HFD-B, LM2M2 and TTY for different values

**Table 5.** Estimations for $^4$He atom$-^4$He dimer scattering lengths $\ell_{\rm sc}$ and inverse wave numbers $\varkappa^{-1}$ corresponding to the excited-state energy $E_{\rm t}^{(1)}$ for the HFD-B, LM2M2 and TTY potentials. The accuracy for the scattering lengths is within $\pm 5$ Å. The grid parameters used for the calculation of $\ell_{\rm sc}$ are: $N_\theta = N_\rho = 502$, $\tau_0 = 0.18$, $\nu = 3.45$ and $\rho_{\max} = 460$ Å.

| Potential | $l_{\max}$ | $\ell_{\rm sc}$ (Å) | $\varkappa^{-1}$ (Å) | Potential | $l_{\max}$ | $\ell_{\rm sc}$ (Å) | $\varkappa^{-1}$ (Å) |
|---|---|---|---|---|---|---|---|
| | 0 | 170[a] 168 | 109 | | 0 | 168 | 113 |
| HFD-B | 2 | 145[a] 138 | 94 | LM2M2/TTY | 2 | 134 | 98 |
| | 4 | 135 | 93 | | 4 | 131 | 96 |

[a] Results from [25] for a grid with $N_\theta = N_\rho = 320$ and $\rho_{\max} = 400$ Å.

**Table 6.** Phase shift $\delta_0^{(l_{\max})}$ results (in degrees) for the HFD-B potential for various c.m. energies $E$ (in mK). The grid parameters used are: $N_\theta = N_\rho = 502$, $\tau_0 = 0.18$, $\nu = 3.45$, and $\rho_{\max} = 460$ Å.

| $E$ | $\delta_0^{(0)}$ | $\delta_0^{(2)}$ | $\delta_0^{(4)}$ | $E$ | $\delta_0^{(0)}$ | $\delta_0^{(2)}$ | $\delta_0^{(4)}$ | $E$ | $\delta_0^{(0)}$ | $\delta_0^{(2)}$ | $\delta_0^{(4)}$ |
|---|---|---|---|---|---|---|---|---|---|---|---|
| −1.68541 | 359.9 | 359.9 | 359.9 | −1.05 | 299.1 | 308.2 | 309.2 | 0.95 | 262.4 | 272.1 | 273.7 |
| −1.68 | 352.6 | 353.9 | 354.1 | −0.8 | 290.8 | 300.4 | 301.5 | 1.2 | 260.0 | 269.6 | 270.7 |
| −1.65 | 341.7 | 345.0 | 345.4 | −0.55 | 284.4 | 294.2 | 295.4 | 1.45 | 257.8 | 267.3 | 268.4 |
| −1.60 | 330.8 | 337.7 | 338.2 | −0.3 | 279.3 | 289.3 | 290.4 | 1.7 | 255.9 | 265.2 | 266.3 |
| −1.55 | 326.9 | 332.8 | 333.5 | −0.05 | 275.1 | 285.2 | 286.3 | 1.95 | 254.1 | 263.4 | 264.5 |
| −1.50 | 322.4 | 329.0 | 329.8 | 0.2 | 271.4 | 281.3 | 282.5 | 2.2 | 252.5 | 261.7 | 262.7 |
| −1.40 | 315.4 | 323.0 | 323.9 | 0.45 | 268.1 | 277.9 | 279.0 | 2.45 | 251.0 | 260.1 | 261.1 |
| −1.30 | 309.9 | 318.1 | 319.1 | 0.7 | 265.1 | 274.8 | 276.0 | | | | |

**Table 7.** Phase shift $\delta_0^{(l_{\max})}$ results for the LM2M2 potential. The units and grid parameters used are the same as in Table 6.

| $E$ | $\delta_0^{(0)}$ | $\delta_0^{(2)}$ | $E$ | $\delta_0^{(0)}$ | $\delta_0^{(2)}$ | $E$ | $\delta_0^{(0)}$ | $\delta_0^{(2)}$ |
|---|---|---|---|---|---|---|---|---|
| −1.30348 | 359.8 | 359.9 | −0.8 | 304.6 | 313.8 | 0.95 | 267.0 | 276.2 |
| −1.3 | 354.1 | 355.3 | −0.55 | 295.2 | 304.8 | 1.2 | 264.1 | 273.2 |
| −1.25 | 337.9 | 342.3 | −0.3 | 287.9 | 297.7 | 1.45 | 261.5 | 270.6 |
| −1.20 | 330.5 | 336.3 | −0.05 | 282.3 | 292.2 | 1.7 | 259.2 | 268.1 |
| −1.15 | 325.2 | 332.0 | 0.2 | 277.7 | 287.4 | 1.95 | 257.1 | 266.0 |
| −1.10 | 321.1 | 328.5 | 0.45 | 273.7 | 283.2 | 2.2 | 255.3 | 264.0 |
| −1.05 | 317.6 | 325.5 | 0.7 | 270.1 | 279.5 | 2.45 | 253.6 | 262.3 |

**Table 8.** Phase shift $\delta_0^{(l_{\max})}$ results for the TTY potential. The units and grid parameters used are the same as in Table 6.

| $E$ | $\delta_0^{(0)}$ | $\delta_0^{(2)}$ | $\delta_0^{(4)}$ | $E$ | $\delta_0^{(0)}$ | $\delta_0^{(2)}$ | $\delta_0^{(4)}$ | $E$ | $\delta_0^{(0)}$ | $\delta_0^{(2)}$ | $\delta_0^{(4)}$ |
|---|---|---|---|---|---|---|---|---|---|---|---|
| −1.30961 | 359.7 | 359.8 | 359.8 | −0.8 | 304.3 | 313.5 | 314.6 | 0.95 | 266.8 | 276.1 | 277.2 |
| −1.308 | 355.9 | 356.8 | 356.9 | −0.55 | 295.0 | 304.6 | 305.7 | 1.2 | 264.0 | 273.1 | 274.2 |
| −1.3 | 350.2 | 352.1 | 352.4 | −0.3 | 287.7 | 297.5 | 298.7 | 1.45 | 261.4 | 270.5 | 271.5 |
| −1.25 | 336.8 | 341.4 | 341.9 | −0.05 | 282.0 | 292.0 | 293.2 | 1.7 | 259.1 | 268.1 | 269.1 |
| −1.2 | 329.7 | 335.7 | 336.4 | 0.2 | 277.5 | 287.3 | 288.4 | 1.95 | 257.0 | 265.9 | 266.9 |
| −1.10 | 320.5 | 328.1 | 329.0 | 0.45 | 273.5 | 283.1 | 284.2 | 2.2 | 255.0 | 263.9 | 265.0 |
| −1.05 | 317.1 | 325.1 | 326.1 | 0.7 | 270.0 | 279.4 | 280.5 | 2.45 | 253.5 | 262.2 | 263.2 |

of $l_{\max}$ are practically the same, especially those for LM2M2 and TTY. The difference between $\delta_0^{(2)}$ and $\delta_0^{(4)}$ is only about 0.5%.

We also compare the values obtained for the He–He$_2$ scattering lengths $\ell_{\rm sc}$ with the corresponding inverse wave numbers $\varkappa^{-1}$ for the trimer excited-state energies. The values of $\varkappa^{-1}$, where $\varkappa = 2\sqrt{(\epsilon_{\rm d} - E_{\rm t}^{(1)})/3}$, with both $E_{\rm t}^{(1)}$ and $\epsilon_{\rm d}$ being given in Å$^{-2}$, are also presented in Table 5. It is seen that these numbers are about 1.3–1.7 times smaller than the respective $^4$He-atom $^4$He-dimer scattering lengths. The situation differs completely from the $^4$He two-atomic scattering problem, where the inverse wave numbers $\left(\varkappa^{(2)}\right)^{-1} = |\epsilon_{\rm d}|^{-1/2}$ are in a rather good agreement with the $^4$He–$^4$He scattering lengths (see Tab. 1).

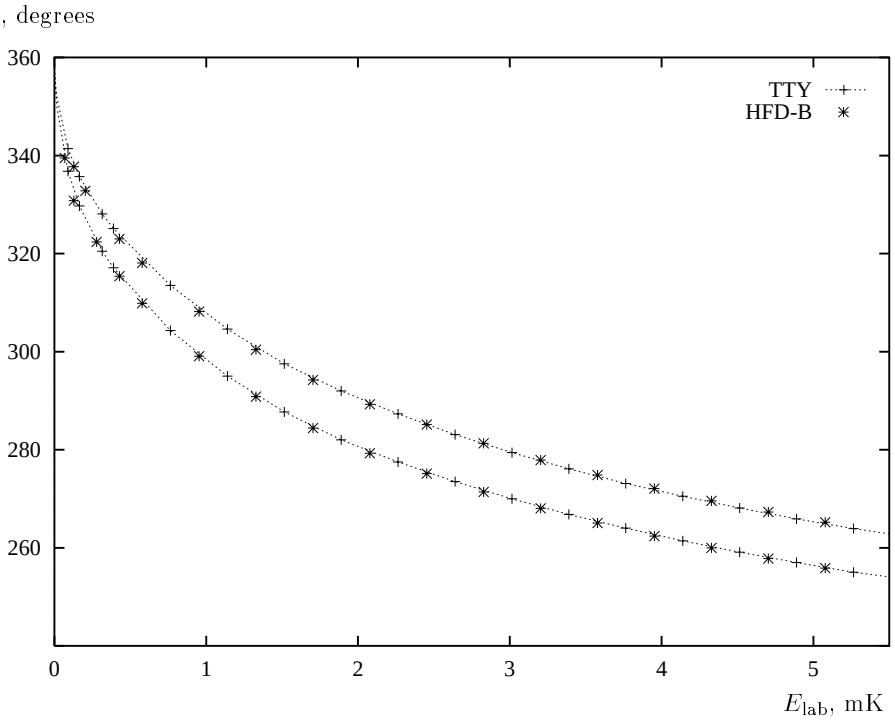


**Fig. 1.** $S$-wave helium-atom helium-dimer scattering phase shifts $\delta_0(E_{\rm lab})$, $E_{\rm lab} = 3(E + |\epsilon_{\rm d}|)/2$, for the HFD-B and TTY $^4$He–$^4$He potentials. The lower curve corresponds to $l_{\max} = 0$ while for the upper one $l_{\max} = 2$.

Such significant differences between $\ell_{\rm sc}$ and $\varkappa^{-1}$ in case of the $^4$He three-atomic system can be attributed to the Efimov nature of the excited state of the trimer, which implies that the effective range $r_0$ for the interaction between the $^4$He atom and the $^4$He dimer is very large as compared to the $^4$He diatomic problem. While the accuracy in our results for the amplitude $a_0(p)$ at $p \approx 0$ is good enough to estimate the scattering length $\ell_{\rm sc}$, we consider it to be still insufficient to extract a definite value of $r_0$.

The authors are grateful to Prof. V.B. Belyaev and Prof. H. Toki for help and assistance in performing the calculations on the supercomputer of the Research Center for Nuclear Physics of Osaka University, Japan. One of the authors (W. S.) would like to thank J.P. Toennies for very interesting discussions stimulating this investigation. Financial support by the Deutsche Forschungsgemeinschaft, the Russian Foundation for Basic Research, and the National Research Foundation of South Africa is gratefully acknowledged.

## Appendix: The potentials used

The general structure of the realistic semi-empirical potentials HFDHE2 [41] and HFD-B [33] developed by Aziz *et al.* is

$$V(x) = \varepsilon\, V_{\rm b}(\zeta) \qquad \text{(A.1)}$$

where $\zeta = x/r_m$ and the term $V_{\rm b}(\zeta)$ reads

$$V_{\rm b}(\zeta) = A\exp(-\alpha\zeta + \beta\zeta^2) - \left[\frac{C_6}{\zeta^6} + \frac{C_8}{\zeta^8} + \frac{C_{10}}{\zeta^{10}}\right] F(\zeta)\,,$$

$x$ is expressed in the same length units as $r_m$ (Å in the present case). The function $F(\zeta)$ is given by

$$F(\zeta) = \begin{cases} \exp\left[-\,(D/\zeta - 1)\right]^2, & \text{if } \zeta \le D \\ 1, & \text{if } \zeta > D\,. \end{cases}$$

In addition to the term $V_{\rm b}(\zeta)$ the LM2M2 potential [36] contains a term $V_{\rm a}(\zeta)$,

$$V(r) = \varepsilon\left\{V_{\rm b}(\zeta) + V_{\rm a}(\zeta)\right\}, \qquad \text{(A.2)}$$

where

$$V_{\rm a}(\zeta) = \begin{cases} A_{\rm a}\left\{\sin\left[\dfrac{2\pi(\zeta-\zeta_1)}{\zeta_2-\zeta_1} - \dfrac{\pi}{2}\right] + 1\right\}, & \zeta_1 \le \zeta \le \zeta_2 \\ 0, & \zeta \notin [\zeta_1, \zeta_2]\,. \end{cases}$$

The parameters for the HFDHE2, HFD-B and LM2M2 potentials are given in Table 9.

The form of the theoretical He–He potential TTY is taken from [37]. This potential reads

$$V(x) = A\left[V_{\rm ex}(x) + V_{\rm disp}(x)\right]$$

**Table 9.** The parameters for the $^4$He−$^4$He Aziz and co-workers potentials used.

| Parameter | HFDHE2 [41] | HFD-B [33] | LM2M2 [36] |
|---|---|---|---|
| $\varepsilon$ (K) | 10.8 | 10.948 | 10.97 |
| $r_m$ (Å) | 2.9673 | 2.963 | 2.9695 |
| $A$ | 544850.4 | 184431.01 | 189635.353 |
| $\alpha$ | 13.353384 | 10.43329537 | 10.70203539 |
| $\beta$ | 0 | −2.27965105 | −1.90740649 |
| $C_6$ | 1.3732412 | 1.36745214 | 1.34687065 |
| $C_8$ | 0.4253785 | 0.42123807 | 0.41308398 |
| $C_{10}$ | 0.178100 | 0.17473318 | 0.17060159 |
| $D$ | 1.241314 | 1.4826 | 1.4088 |
| $A_{\rm a}$ | − | − | 0.0026 |
| $\zeta_1$ | − | − | 1.003535949 |
| $\zeta_2$ | − | − | 1.454790369 |

**Table 10.** The parameters for the $^4$He−$^4$He TTY potential used.

| | | | |
|---|---|---|---|
| $A$ (K) | 315766.2067$^{(a)}$ | $C_6$ | 1.461 |
| $\beta$ $\left((\text{a.u.})^{-1}\right)$ | 1.3443 | $C_8$ | 14.11 |
| $D$ | 7.449 | $C_{10}$ | 183.5 |
| $N$ | 12 | | |

$^{(a)}$The value of $A$ was obtained from the data presented in [37] using, for converting the energy units, the factor $1\ \text{K} = 3.1669 \times 10^{-6}$ a.u.

where $x$ stands for the distance between the $^4$He atoms given in atomic length units. (Following [37] in converting the length units we used 1 a.u. = 0.52917 Å.) The function $V_{\rm ex}$ has the form

$$V_{\rm ex}(x) = D\, x^p \exp(-2\beta x)$$

with $p = \dfrac{7}{2\beta} - 1$, while the function $V_{\rm disp}$ reads

$$V_{\rm disp}(x) = -\sum_{n=3}^{N} C_{2n}\, f_{2n}(x)\, x^{-2n}\,.$$

The coefficients $C_{2n}$ are calculated *via* the recurrency relation

$$C_{2n} = \left(\frac{C_{2n-2}}{C_{2n-4}}\right)^3 C_{2n-6}\,,$$

and the functions $f_{2n}$ are given by

$$f_{2n}(x) = 1 - \exp(-bx) \sum_{k=0}^{2n} \frac{(bx)^k}{k!}$$

where

$$b(x) = 2\beta - \left[\frac{7}{2\beta} - 1\right] \frac{1}{x}.$$

The parameters of the TTY potential are given in Table 10.

## References


1. J.P. Toennies, K. Winkelmann, J. Chem. Phys. **66**, 3965 (1977).
2. M.V. Rama Krishna, K.B. Whaley, Phys. Rev. Lett. **64**, 1126 (1990).
3. K.K. Lehman, G. Scoles, Science **279**, 2065 (1998).
4. S. Grebenev, J.P. Toennies, A.F. Vilesov, Science **279**, 2083 (1998).
5. V. Efimov, Nucl. Phys. A **210**, 157 (1973).
6. F. Luo, G.C. McBane, G. Kim, C.F. Giese, W.R. Gentry, J. Chem. Phys. **98**, 3564 (1993).
7. F. Luo, C.F. Giese, W.R. Gentry, J. Chem. Phys. **104**, 1151 (1996).
8. W. Schöllkopf, J.P. Toennies, Science **266**, 1345 (1994).
9. U. Buck, H. Meyer, J. Chem. Phys. **84**, 4854 (1986).
10. O. Echt, K. Sattler, E. Recknagel, Phys. Rev. Lett. **47**, 1121 (1981).
11. W. Schöllkopf, J.P. Toennies, J. Chem. Phys. **104**, 1155 (1996).
12. S.W. Rick, D.L. Lynch, J.D. Doll, J. Chem. Phys. **95**, 3506 (1991).
13. V.R. Pandharipande, J.G. Zabolitzky, S.C. Pieper, R.B. Wiringa, U. Helmbrecht, Phys. Rev. Lett. **50**, 1676 (1983).
14. R.N. Barnett, K.B. Whaley, Phys. Rev. A **47**, 4082 (1993).
15. M. Lewerenz, J. Chem. Phys. **106**, 4596 (1997).
16. R. Guardiola, M. Portesi, J. Navarro, LANL `e-print physics/9904037`.
17. T. González-Lezana, J. Rubayo-Soneira, S. Miret-Artés, F.A. Gianturco, G. Delgado-Barrio, P. Villareal, Phys. Rev. Lett. **82**, 1648 (1999).
18. B.D. Esry, C.D. Lin, C.H. Greene, Phys. Rev. A **54**, 394 (1996).
19. E. Nielsen, D.V. Fedorov, A.S. Jensen, J. Phys. B **31**, 4085 (1998) (LANL `e-print physics/9806020`).
20. S. Nakaichi-Maeda, T.K. Lim, Phys. Rev. A **28**, 692 (1983).
21. Th. Cornelius, W. Glöckle, J. Chem. Phys. **85**, 3906 (1986).
22. J. Carbonell, C. Gignoux, S.P. Merkuriev, Few-Body Systems **15**, 15 (1993).
23. V. Roudnev, S. Yakovlev, LANL `e-print physics/9910030`.
24. P.F. Bedaque, H.-W. Hammer, U. van Kolck, Nucl. Phys. A **646**, 444 (1999) (LANL `e-print nucl-th/9811046`).
25. E.A. Kolganova, A.K. Motovilov, S.A. Sofianos, J. Phys. B. **31**, 1279 (1998) (LANL `e-print physics/9612012`).
26. T. Frederico, L. Tomio, A. Delfino, A.E.A. Amorim, Phys. Rev. A **60**, R9 (1999).
27. A.K. Motovilov, E.A. Kolganova, Few-Body Systems Suppl. **10**, 75 (1999) (LANL `e-print physics/9810006`).
28. E.A. Kolganova, A.K. Motovilov, Phys. Atom. Nucl. **62**, 1179 (1999) (LANL `e-print physics/9808027`).
29. G.C. Hegerfeldt, T. Köhler, LANL `e-print quant-ph/0002054`.
30. P.O. Fedichev, M.W. Reynolds, G.V. Shlyapnikov, Phys. Rev. Lett. **77**, 2921 (1996).
31. E.A. Kolganova, A.K. Motovilov, S.A. Sofianos, Phys. Rev. A. **56**, R1686 (1997) (LANL `e-print physics/9802016`).
32. A.K. Motovilov, S.A. Sofianos, E.A. Kolganova, Chem. Phys. Lett. **275**, 168 (1997) (LANL `e-print physics/9709037`).

33. R.A. Aziz, F.R.W. McCourt, C.C.K. Wong, Mol. Phys. **61**, 1487 (1987).
34. S.P. Merkuriev, A.K. Motovilov, Lett. Math. Phys. **7**, 497 (1983).
35. S.P. Merkuriev, A.K. Motovilov, S.L. Yakovlev, Theor. Math. Phys. **94**, 306 (1993).
36. R.A. Aziz, M.J. Slaman, J. Chem. Phys. **94**, 8047 (1991).
37. K.T. Tang, J.P. Toennies, C.L. Yiu, Phys. Rev. Lett. **74**, 1546 (1995).
38. A.K. Motovilov, Vest. Leningr. Univ. **22**, 76 (1983).
39. L.D. Faddeev, S.P. Merkuriev, *Quantum scattering theory for several particle systems* (Kluwer Academic Publishers, Doderecht, 1993).
40. S.P. Merkuriev, C. Gignoux, A. Laverne, Ann. Phys. (N.Y.) **99**, 30 (1976).
41. R.A. Aziz, V.P.S. Nain, J.S. Carley, W.L. Taylor, G.T. McConville, J. Chem. Phys. **79**, 4330 (1979).
42. A.A. Samarsky, *Theory of difference schemes* (in *Russian*) (Nauka, Moscow, 1977).
43. The NIST Reference on Constants, Units, and Uncertainty. Converion factors for energy equivalents (`http://physics.nist.gov/cuu/Constants/energy.html`).
44. Y. Kagan, A.E. Muryshev, G.V. Shlyapnikov, Phys. Rev. Lett. **81**, 933 (1998).
45. D. Blume, C.H. Green, J. Chem. Phys. (to appear).
46. N. Levinson, K. Dan. Vidensk. Selsk. Mat. Fys. Medd. **25**, 9 (1949).